THE JOURNAL OF PHYSICAL CHEMISTRY C

Article

pubs.acs.org/JPCC

Anaerobic Oxidation of Methane to Methyl Radical in NTf_2-Based Ionic Liquids

Zhe Wang, Anil Kumar, Michael D. Sevilla, and Xiangqun Zeng*

Department of Chemistry, Oakland University, Rochester, Michigan 48309, United States

Supporting Information

ABSTRACT: In this report, we show that at the ionic liquid (IL)/Pt electrode interface, the C−H bond in methane can be activated and abstracted in situ to form methyl radical by electrochemically generated bis((trifluoromethyl)sulfonyl)-amide ([NTf_2]) radicals from the ionic liquid, 1-butyl-1-methylpyrrolidinium bis((trifluoromethyl)sulfonyl)amide ([Bmpy][NTf_2]). DFT modeling supports the abstraction of hydrogen from CH_4 by the NTf_2• radical resulting in the formation of a methyl radical that then reacts with the IL to form the CF_3• radical and molecular products, CF_3CF_3 and CF_3H. This work thus provides a new pathway of controlled activation of the C−H bond of methane anaerobically at low potential in a neutral condition at room temperature which can have important applications such as organic electrochemistry and preparative-scale organic electrochemical synthesis.

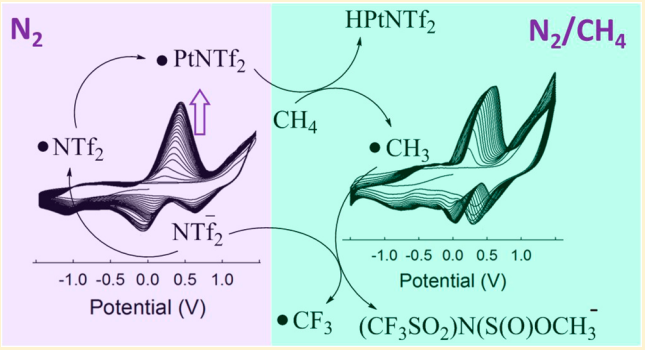

INTRODUCTION

Methane is one of the most abundant organic molecules in nature and the main component of natural gas. Methane is also a powerful greenhouse gas that is far more effective at trapping heat in the atmosphere than carbon dioxide, significantly impacting climate change.[1,2] Methane is found both below ground and under the sea floor. The vast reserve of methane in nature makes it an ideal chemical feedstock for the production of liquid fuels and chemicals. However, methane is underutilized since the C−H bond in methane is regarded as one of the strongest C−H bonds (104 kcal/mol). Currently the economical and sustainable strategies for the controlled oxidation of methane are lacking. Typically methane can be oxidized by strong oxidizing acids such as H_2SO_4[3] and OsO_4/$NaIO_4$[4] in the presence of metal catalysts. Anaerobic oxidation of methane mediated by consortia of archaea and sulfate-reducing bacteria was reported. Recently, it was shown that direct anaerobic oxidation of methane can be coupled with sulfate reduction or coincided with denitrification of nitrite/nitrate.[2,5−8] The one-electron oxidation of methane is particularly unfavorable from a thermodynamic standpoint, and therefore, the generation of methyl radicals requires the use of rather strong oxidants and/or high temperatures. In the past decades, many catalysts for methane oxidation were reported;[3,6,9] however, they suffer from some combinations of low selectivity, catalyst instability, extreme reaction conditions (strong acidic media, high temperature, and high pressure),[10−12] which hinder their uses at the industrial scale.

The rate-limiting step of methane oxidation is dissociative of chemisorbed CH_4 by breaking one of the C−H bonds via the Eley−Rideal-type mechanism.[1] In this work, we demonstrate a new approach via electrochemically generated reactive radical species from an ionic liquid (IL) at the Pt electrode for selective activation and functionalization of C−H bonds in methane. ILs containing organic cation or anions have been shown to act as "green" reaction media for various chemical reactions.[13−15] Redox reactions and fragmentation of constituent ions in ILs can be explored to selectively generate reactive radicals to promote the oxidation of the methane.[16] Furthermore, ILs could provide an anaerobic (oxygen-free) environment. The flexibility and tunability of ILs enable new reaction pathways since the rate and selectivity of a chemical reaction can be remarkably and reversibly changed by electrochemical polarization of the electronic conductive catalyst (Pt) in an IL electrolyte (i.e., an ionic conductive medium). The solubility of methane in many ILs is also higher than many other solvents. These features can increase the amount of methane adsorption and the rate of methane oxidation at the same time. Thus, we rationally selected an IL with fluorine-containing anion bis(trifluoromethylsulfonyl)imide ([NTf_2]) and a bulky quaternary ammonium cation, 1-butyl-1-methylpyrrolidinium ([Bmpy]). The bulky [Bmpy] cation forces the anions away from the cation, and the delocalization of the negative charge along the −S−N−S− core of the NTf_2^- anion also reduces the cation and anion interaction. Both factors could facilitate NTf_2^- anion reactivity with Pt surface under electrochemical conditions. The methane oxidation processes by bisulfate and other sulfides have been reported at anaerobic condition

Received: January 6, 2016
Revised: May 20, 2016
Published: May 25, 2016

DOI: 10.1021/acs.jpcc.6b00153
J. Phys. Chem. C 2016, 120, 13466−13473

before,[17−19] and the NTf_2^- based complex catalyst has high activity to active C−H and C−C bonding.[20−22] Our recent work discovered that we can directly oxidize the NTf_2^- anion to form a radical electrocatalyst on the platinum electrode at the anaerobic condition.[23] The in situ generated radical catalyst was shown to catalytically and selectively promote the electrooxidation of methanol to form the methoxyl radical, at a potential drastically less positive in the presence of the NTf_2• radical. In this report, we demonstrate that the in situ electrochemically generated NTf_2• radical from [Bmpy][NTf_2] can subsequently activate the C−H bond in methane to form methyl radicals that then react with the IL to form CF_3• and molecular products, CF_3CF_3 and CF_3H. The CF_3• radical is of tremendous significance for organofluorination.[24] With combined electrochemical studies of DFT and NMR spectroscopic characterization, a multiple step mechanism was proposed. This study provides strong evidence of a promising flexible method using the unique properties of ILs not only for anaerobic oxidation of methane but also as a potential medium to generate electrocatalysts for many other hydrocarbon conversions.

EXPERIMENTAL SECTIONS

The chemicals and reagents, structure, and physical properties of the ionic liquids used in this study, details of the electrochemical experiments, and the supporting data of Figures S1−S9 are described in the Supporting Information.

RESULTS AND DISCUSSION

DFT Calculations of NTf_2 Radical and Methane Interactions. The C−H bond of methane is relatively strong and difficult to oxidize. We characterize possible pathways of methane oxidation in the [Bmpy][NTf_2] using density function theory calculations (DFT). Advances in DFT have made it possible to elucidate the elementary steps and mechanisms in chemical processes that would be difficult to explore experimentally. The electrochemical one electron oxidation of NTf_2^- anion has been reported in our earlier work to produce the NTf_2• radical species.[23] Using the Spartan 10 program set,[25] we have performed a test of the reaction of this radical species with methane employing the DFT with the B3LYP functional and a 6-31G* basis set to gain initial reasonable estimates of the likelihood of the reaction shown in eq 1.

$$\text{Pt—NTf}_2\bullet + \text{CH}_4 \rightarrow \text{HPtNTf}_2 + \text{CH}_3\bullet \quad (1)$$

The NTf_2 radical was first geometry optimized and C−H bond in methane was placed so that a C−H bond was directed at the N radical site in NTf_2• at a N−H distance of 2.6 Å (Figure 1). The N−H bond length was incrementally shortened in 0.1 Å excrements to 0.8 Å. The minimum was found at 1.0 Å, and a subsequent full optimization found the true minimum at 1.032 Å (Figure 1). The abstraction of the hydrogen atom from methane is downhill energetically (−7.1 kJ/mol) and leaves the H-NTf_2 neutral molecule and a methyl radical. The activation barrier was found to be ca. 37 kJ/mol, which is low enough for a rapid reaction to occur. More accurate full thermodynamic calculations were then performed using the Gaussian09 program set[26] for the free energy change for the overall reaction using B3LYP/6-311++G** which gives a more favored result with ΔG° = −12.1 kJ/mol in the gas phase and a substantially more favorable value in the IL environment of ΔG° = −21.6 kJ/mol using IE-PCM with a dielectric constant of 11.7 reported for [Bmpy][NTf_2]. Thus, the C−H bond of methane is predicted to be abstracted by the NTf_2• radical formed at a low electrochemical potential. On deprotonation of the H-NTf_2, the ionic liquid NTf_2 would be restored and could act as a catalyst in the oxidation of methane except for the fact that the methyl radical is predicted to react with the NTf_2 (vide infra).

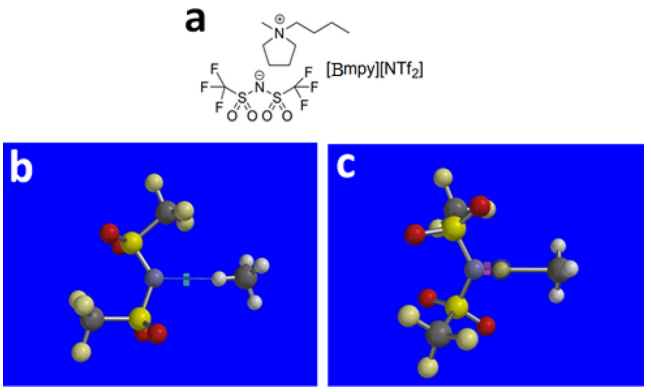

Figure 1. DFT calculations of NTf_2 radical and methane interactions. (a) Structure of [Bmpy][NTf_2]. (b) The optimized geometry of NTf_2 radical at DFT/B3LYP/6-31G* at a N−H initial separation of 2.6 Å. (c) The optimized geometry at the minimum in energy at N−H distance of 1.032 Å showing a methyl radical and the $HNTf_2$ molecule. This abstraction reaction is favored energetically by 7.1 kJ/mol with a ca. 37 kJ/mol barrier height. More accurate full thermodynamic calculations for the free energy change for the overall reaction using B3LYP/6-311++G** gives a more favored result with $\Delta G^{\circ(\text{gas})}$ = −12.1 kJ/mol. Using integral equation formalism of the polarized continuum model (IEF-PCM) with a dielectric constant of 11.7 of the IL, we find an even more favorable result of $\Delta G^{\circ(\text{IL})}$ = −21.6 kJ/mol.

Anaerobic Oxidation of Methane by in situ Electrochemical Generated NTf_2• Radical in [Bmpy][NTf_2]. Figure 2a shows the cyclic voltammetry (CV) results of redox processes at Pt electrode in [Bmpy][NTf_2] under nitrogen atmosphere. As discussed in our recent report, NTf_2^- anion acts as a weak ligand. At room temperature, NTf_2^- can be oxidized to a highly active NTf_2• free radical at anodic potential, which subsequently forms the Pt-NTf_2• adsorbate.[23] As shown in Figure 2, peaks B and B′ are explained as the results of the reversible oxidation and reduction of the Pt-NTf_2• adsorbate. The peak A/A′ is the result of the NTf_2^- anion being oxidized at 1.2 V (peak A) to the NTf_2• radical in which some of them are being reduced in the cathodic scan (peak A′) and some of them can subsequently adsorb at the Pt electrode leading to a redox peak A/A′ at 0.5 V. However, at initial cycles, the NTf_2• radical generated can diffuse away due to a maximum concentration gradient near the IL-electrode interface. With subsequent potential cycling, the increasing amount of NTf_2• accumulated near the IL-Pt electrode interface and resulted in the increasing of peak B/B′ currents. Consistent with our recent work,[23] the Pt-NTf_2• formation is favored by the higher anodic potentials at the platinum electrode, as seen in Figure S2−S3 (the results of potential sweep at variable potential windows, Supporting Information). Figure 2b shows the multiple cyclic voltammograms in the presence of methane. One significant difference when compared with Figure 2a is that the peak B/B′ appears in the second and subsequent potential cycles, and there is an obvious peak shift of both peak A/A′ and B/B′ during the multiple potential cycle experiments. We rationalize that the Pt-NTf_2•

DOI: 10.1021/acs.jpcc.6b00153
J. Phys. Chem. C 2016, 120, 13466−13473

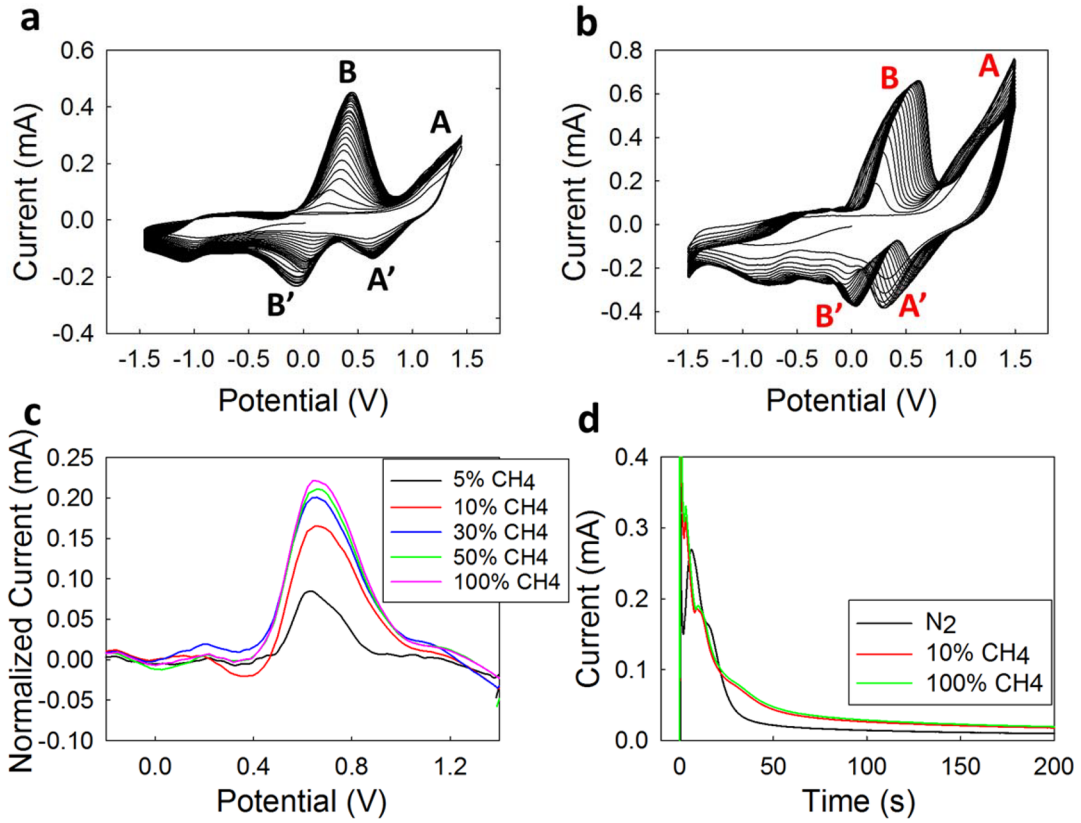

Figure 2. (a) CV in nitrogen, and (b) CV in methane. (c) Normalized methane anodic current at different methane concentrations using the modified platinum electrode in nitrogen (i.e., first oxidizing NTf_2^- anion to form the Pt-NTf_2• radical surface adsorbate in the nitrogen conditions until the peak current reaches a constant and then methane is introduced at various concentrations in nitrogen) (see the Supporting Information for details). (d) Current vs time curves when potential is stepped to 0.6 V when the electrochemical system is exposed to nitrogen, 10% methane, and 100% methane, respectively. Scan rate for CVs is 500 mV s^{-1}. Pt electrode and [Bmpy][NTf_2] electrolyte.

adsorbate not only can be reduced but also can facilitate the abstraction of hydrogen from the C−H bond of methane at low potential around 0.6 V. The Pt-NTf_2• adsorbate is rendered significantly more electrophilic compared to analogous halide species with resulting profound effects on decreasing the potential of electrochemical process.[27] The current of peak B increased gradually and peak potential shifted anodically in the subsequent scans until reaching to ∼0.6 V. These results support the DTF study that methane is being oxidized to a methyl radical, which participates in the NTf_2^- redox processes in peak A and peak B which led to the peak potential shifts. As shown in Figure S4 at the gold electrode, electrochemical oxidation of NTf_2^- was not observed and there was no NTf_2 adsorbed on the Au electrode. There was no redox peak observed in the cyclic voltammogram in N_2 or in the presence of CH_4 on the gold electrode. It confirmed that gold is not a catalytic electrode for methane oxidation. Pt was widely used as the catalyst for the methane oxidation in aqueous and traditional nonaqueous electrolytes[28] since it has a high methane adsorption ratio by formation of Pt-H bonds. Our early work also showed that Pt has high activity as the coordination center to bond with species such as the NTf_2• radical to form the Pt NTf_2• radical catalyst for abstraction of hydrogen from methanol.[23]

We performed linear voltammetry in which we first oxidized the NTf_2^- anion to form the Pt-NTf_2• radical surface adsorbates in anaerobic conditions (i.e., pure nitrogen), and then we introduce methane at various concentrations maintaining anaerobic conditions. Figure 2c shows that the anodic currents enhanced with an increase in the methane concentrations around 0.65 V. It indicated that the electrochemically derived active NTf_2• could in situ oxidize methane at the platinum surface in an anaerobic condition. And this process is not a diffusion-controlled process, as methane concentration and peak current follows a nonlinear relationship. It was further proved by the chronoamperometry results (Figure 2d and detailed in Figure S5). It shows very different transient behaviors in the presence of methane from those in pure nitrogen conditions. With increased methane concentrations, the current decay processes show several relaxation processes. The relaxation curves do not obey the conventional Cottrell "exponential decay" equations that describe the diffusion-controlled process. Here, the surface-confined redox reaction occurred in an irreversible multiple step consecutive process.[29,30] These kinds of relaxation curves followed multiple slower processes and are similar to those observed in other complexes and disordered systems[31] such as conductive polymer interfaces.[32,33]

DFT Study of Methyl Radical Reactions with the Ionic Liquid. It is well-known that the methyl radical has a short lifetime in organic systems. For example, the rate constant for the methyl radical abstraction from acetone is reported to be 1.3×10^7 L mol^{-1} s^{-1}, which corresponds to a half-life of 0.1 μs at 1 M acetone.[34] The addition reactions of methyl radicals with molecular oxygen are also very rapid and would be on a larger scale than the μs time scale.[35] Currently no kinetics have been done on these reactions in ILs, but recent studies shows that cation radicals, such as that for anthracene, display similar

DOI: 10.1021/acs.jpcc.6b00153
J. Phys. Chem. C 2016, 120, 13466−13473

lifetimes in ILs as in other organic solvents.[36] Thus, the kinetics of methyl radical in the IL would be similar to those found in organic systems likely on the microsecond time frame. Methyl radical is very reactive and can act as either a strong oxidant or a strong reductant. Using the same DFT approach, we studied the possible reactions of the methyl radical formed in reaction 1 with the NTf_2^- anion and found that the methyl radical readily adds to the oxygen atoms in NTf_2^- and forms a strong C−O bond that creates an overall unstable species. This adduct leads to an energetically downhill fragmentation (ΔG^o = −24.0 kJ/mol (gas phase) and ΔG^o = −38.7 kJ/mol (IL dielectric constant, 11.7[37]) of the NTf_2 framework by CF_3 radical loss (see Figure 3) and eq 2.

$$CH_3\bullet + N(SO_2CF_3)_2^- \rightarrow CF_3\bullet + (CF_3SO_2)N(S(O)OCH_3)^- \quad (2)$$

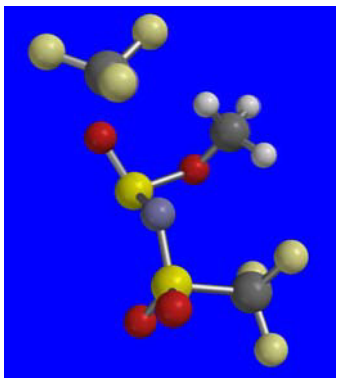

Figure 3. Optimized geometry (DFT/B3LYP 6-31G*) after methyl radical attachment to an NTf_2^- oxygen. The C−O bond length is 1.432 Å, and the CF_3 radical is lost at 3.7 Å. This fragmented form is 29.0 kJ/mol lower in energy than the total of the separate methyl radical and NTf_2^- species. A full thermodynamic calculation for the free energy change for the overall reaction using B3LYP/6-311++G** in the gas phase also shows a favored reaction with ΔG^o = −24.0 kJ/mol. This reaction is predicted to be substantially more favorable in the ionic liquid, ΔG^o = −36.8 kJ/mol.

The $CF_3\bullet$ formed in eq 2 is found to be able to abstract from methane, shown in eq 3. The full thermodynamic calculation for the free energy change for eq 3 was computed and was found to be slightly favored with ΔG^o = −4.6 kJ/mol at the 6-311++G** B3LYP level but this value is increased in the ionic liquid environment to ΔG^o = −12.8 kJ/mol, employing an integral equation formalism polarizable continuum model (IE-PCM) with a dielectric constant of 11.7 for [Bmpy][NTf_2][37]).

$$CH_4 + CF_3\bullet \rightarrow HCF_3 + CH_3\bullet \quad (3)$$

Thus, $CF_3\bullet$ and CH_4 are energetically favored to form $CH_3\bullet$ and HCF_3. The $CF_3\bullet$ formed by attack of the methyl radical on the NTf_2 anion will then readily abstract a hydrogen atom from methane to produce additional HCF_3 (found experimentally, see the MS and NMR study below), as well as form additional $CH_3\bullet$ which can further react in a cyclic manner.

NMR and GC/LC−MS Characterization of Anaerobic Methane Oxidation in [Bmpy][NTf_2]. Electrochemical reactions identical to those shown in Figure 2b were performed. The gas phase products of voltammetric reactions were collected (see the Supporting Information for experimental details and Figure S1 for the experimental setup) and were analyzed by gas chromatography/mass spectroscopy (GC/MS) and nuclear magnetic resonance (NMR). F^{19}NMR spectrum of the final products, which were collected by dry ice cold trap, confirmed only two chemicals with the F element, which were assigned as HCF_3 and CF_3CF_3, respectively (F^{19}: δ = −68.0 and −78.1; C^{13}: δ = 115 and 125).[38,39] GC/MS analysis of the products independently confirmed this result, and we found masses appropriate for CF_3CF_3 (m/z 138) and HCF_3 (m/z 70). We note that these products are those expected result of reaction shown as eqs 8 to 10 and add evidence for these reaction mechanisms in which Pt-NTf_2 and CH_3 free radicals form on the polarized platinum surface, and CH_3 free radical attack on the S-CF_3 bonding forms the CF_3 radical as predicted by our DFT calculations.[40,41]

The mechanism of the reaction in the presence of methane is proposed as follows:

$$NTf_2^- - e^- \rightarrow NTf_2\bullet \quad (4)$$

$$NTf_2\bullet + Pt \rightarrow PtNTf_2\bullet \text{ adsorbate} \quad (5)$$

$$PtNTf_2\bullet (ads) + e^- \rightarrow PtNTf_2^- (ads) \quad (6)$$

$$PtNTf_2\bullet (ads) + CH_4 (ads) \rightarrow HPtNTf_2 + CH_3\bullet \text{ (shift of peak B/B}') \quad (7)$$

$$CH_3\bullet + N(SO_2CF_3)_2^- \rightarrow CF_3\bullet + (CF_3SO_2)N(S(O)_2OCH_3^-) \quad (8)$$

$$CF_3\bullet + CH_4 \rightarrow HCF_3 + CH_3\bullet \quad (9)$$

$$2CF_3\bullet \rightarrow CF_3CF_3 \quad (10)$$

$$\text{Net: } 3CH_4 + 5NTf_2^- \rightarrow 3(CF_3SO_2)N(S(O)OCH_3)^- + 2\,HNTf_2 + HCF_3 + CF_3CF_3 \quad (11)$$

The oxidative and reductive cleavages of fragmentation of NTf_2^- anions leads to the molecular products CF_3CF_3 and CF_3H, and the mole ratio of these two products obtained by F^{19}NMR was close to 1:1. The other product predicted $(CF_3SO_2)N(S(O)OCH_3)^-$ would be easily converted to CH_3OH, CF_3SO_2NH, and SO_2 via a simple hydrolysis reaction.[42,43]

Kinetic Studies of Anaerobic Oxidation of Methane at the IL-Pt Electrode Interface. As discussed above that the methane oxidation by the in situ generated Pt-$NTf_2\bullet$ radical catalyst involves complicated multiple-step reactions, the kinetic of these processes were investigated by varying the methane concentrations and studying the relationship of peak B currents vs methane concentrations by CV. As discussed above, the first anodic potential scan to 1.0 V oxidized the NTf_2^- anion to form the $NTf_2\bullet$ radical which can adsorb at the Pt surface to form the $PtNTf_2\bullet$ radical catalyst. This radical catalyst initiates the methane oxidation showing in the subsequent second potential cycle. As discussed in the DFT study in Figure 3b, the peak B involves the abstraction of hydrogen from the C−H bond of methane by the adsorbate $PtNTf_2\bullet$ on the Pt surface. The electrode was preactivated by undergoing six cycles of CV under nitrogen to lay down a consistent catalytic layer of $NTf_2\bullet$-Pt on the electrode for each concentration measurement. The increase in peak current from

DOI: 10.1021/acs.jpcc.6b00153
J. Phys. Chem. C 2016, 120, 13466−13473

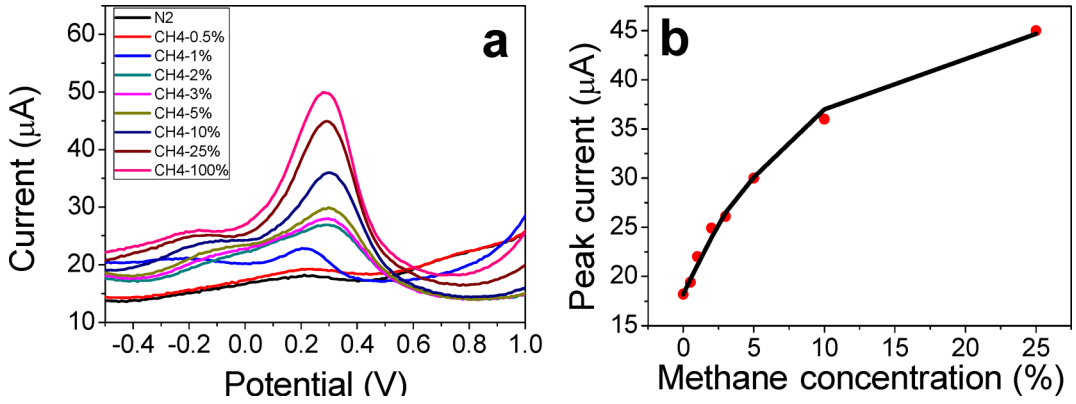

Figure 4. (a) The kinetics study of methane anaerobic oxidation, and the voltammograms of anaerobic oxidation of methane at different methane concentrations (500 mV/s scan rate). The electrode was preactivated by undergoing six cycles of CV under the nitrogen condition to lay down a consistent catalytic layer of $PtNTf_2$● on the electrode for each methane concentration measurement. (b) The plot of peak current vs volume % methane concentrations in (a). The black line is the fitting curve by the Langmuir–Hinshelwood mechanism for the methane/IL/platinum (gas/liquid/solid) interface.

the current found after preactivation was reported as the catalytic current. As shown in Figure 4a, the anodic peak B currents increase with methane concentrations, indicating the peak B current signal is directly related to the amount of methane available at the Pt electrode interface. A nonlinear relationship of peak B currents and methane concentrations is shown in Figure 4b. With the increase of methane concentrations, the sensitivity (slopes in Figure 4b) decreases from about 3.8 μA/% to 0.6 μA/% as the concentration of methane increases from 0% to 25% (v/v). As discussed above, the methane anaerobic oxidation in the Pt/IL system involves adsorption of methane and anion of IL, and this process facilitates the methane oxidation. Thus, the Langmuir–Hinshelwood theory was applied to obtain the kinetic rate constants of various steps involving methane oxidation.

The mass balance at the electrode surface is given by eqs 10 and 11 below

$$\Gamma_T = \Gamma_{CH4} + \Gamma_{IL} + \Gamma_{Pt} \tag{12}$$

or

$$1 = \theta_{CH4} + \theta_{IL} + \theta_{Pt} \tag{13}$$

Where Γ_i represents the surface coverage of a specific species i (in mol/cm^2), $\theta_i = \Gamma_i/\Gamma_T$ is the relative surface coverage of species i and Γ_T is the total surface coverage of all species.

The rate of adsorption (V_{ad}) and desorption (V_{de}) of CH_4 and IL at the electrode can be described by the following eqs 14 to 16:

$$V_{adCH_4} = k_1 C_{CH4}(1 - \theta_{CH_4} - \theta_{IL}) \tag{14}$$

$$V_{adIL} = k_2 C_{IL}(1 - \theta_{CH_4} - \theta_{IL}) \tag{15}$$

$$V_{deCH_4} = k_1'\theta_{CH_4} \tag{16}$$

$$V_{deIL} = k_2'\theta_{IL} \tag{17}$$

where k and k' are the reaction rate constants. C_{CH4} is concentration of methane, and C_{IL} is the concentration of IL, in our case.

$$K = \frac{k}{k'} \tag{18}$$

When the rate of adsorption is in equilibrium with the rate of desorption for each species, the resulting equations can be solved simultaneously for θ_{CH4} and θ_{IL} as shown in the following equations. K_1 and K_2 are the equilibrium constants of methane adsorption and IL adsorption, respectively.

$$\theta_{CH_4} = \frac{K_1 C_{CH_4}}{1 + K_1 C_{CH_4} + K_2 C_{IL}} \tag{19}$$

$$\theta_{IL} = \frac{K_2 C_{IL}}{1 + K_1 C_{CH_4} + K_2 C_{IL}} \tag{20}$$

The rate of methane oxidation is equal to

$$V_3 = k_3 \theta_{CH_4} \theta_{IL} \tag{21}$$

where k_3 is the rate constant of methane oxidation. The total Faradaic current density is the sum of currents due to reactions of IL electrolysis and methane oxidation:

$$J_F = j_{oxidation} + j_{IL} = F\Gamma_T(V_3 + V_2) \tag{22}$$

So we can get the total current of this reaction:

$$j_{total} = \left(\frac{K_1 K_2 k_3 C_{CH_4} C_{IL}}{(1 + K_1 C_{CH_4} + K_2 C_{IL})^2}\right) F\Gamma + j_{EDL} \tag{23}$$

j_{EDL} is the double layer charging current in the IL, which was found in most of the IL system.[2,44,45] In our experiments, it can be considered as a constant because the Faradaic current is significantly bigger than the electric double layer charging current. The change of charging current due to the presence of methane was also very small.

The current density of methane oxidation can be expressed as

$$j_{total} = \frac{\Gamma F K_1 K_2 k_3 C_{CH_4}}{(1 + K_1 C_{CH_4} + K_2)^2} + j_{EDL} \tag{24}$$

On the basis of the results from cyclic voltammetry, we used the current of the sixth cycle in the nitrogen condition without any redox processes as our background signal. The double layer charging current can be estimated from CV at the sixth cycle in pure nitrogen condition ($C_{CH4} = 0$) to be 18.2 μA. Eq 24 was input into Origin 8.0 nonlinear software.

DOI: 10.1021/acs.jpcc.6b00153
J. Phys. Chem. C 2016, 120, 13466–13473

From the fitting result, the relationship between the peak current and methane concentration is as follows:

$$I_{peak} = \frac{9.35C_{CH_4}}{(0.05C_{CH_4} + 1.74)^2} + 18.2 \quad (r^2 = 0.99479) \tag{25}$$

On the platinum surface, the methane adsorption constant K_1 is 0.05 ($\%^{-2}$) and the constant of the ionic liquid reaction (K_2) is about 0.74 ($\%^{-2}$). If Γ_T is 1, k_3 is about 0.0026($\%^{-2}$). Comparing with the electrochemical process of IL on the electrode surface, the three-phase reaction of methane oxidation k_3 has the smallest rate constant,[46] which may explain the oxidation peak shift to higher potential at high methane concentration.

Effects of Ionic Liquid Structures on the in Situ Generated Precursor. Table S1 listed several other ionic liquids with different structures that were studied under the same experimental conditions. The current at the potential of peak B was measured and compared. The rate constant of k_3 of methane oxidation was summarized in Table 1. From the CV result, there were no reactions between other types of ionic liquids and methane. Only those with the NTf_2^- anion species show activity. Obviously, there is significant influence of the cation to the reaction rates. [Bmpy][NTf_2] gives the highest response for methane electro-oxidation based on the electrochemical voltammetry results. It is likely the larger cation $[C_{10}mpy]^+$ with the longer side-chain of ten carbons blocked the active site of platinum surface and decreased the activity of NTf_2^-. The ion activities are also constrained by the viscosity of the ionic liquids. The free radical is expected to diffuse more slowly in ionic liquid solvents, and the diffusion coefficients of the free radical vary with the ionic liquid properties. Although the viscosity of [Bmim][NTf_2] is similar to [Bmpy][NTf_2], the rate of methane oxidation is slower in [Bmim][NTf_2], suggesting the cation effects. Because of the planar structure of cation $[Bmim]^+$, the $[Bmim]^+$ orientation in the ionic liquid double layer is different from that of the [Bmpy][NTf_2], which in turn affects the double layer capacitance during the potential scan.[47] This affects the methane oxidation current even though the mechanism is likely the same. Given the complexity of [Bmim][NTf_2] as solvents, emerging phenomena occurring in ILs such as microheterogeneity or fractional Stokes−Einstein behavior cannot be ruled out. These results support that the NTf_2^- plays the key role in anaerobic methane oxidation.

Table 1. Value of k_3 in Different Ionic Liquids

		cation			
$k3$ ($\%^{-2}$)		Bmpy	C10mpy	Bmim	N_{4441}
anion	NTf_2	**0.0026**	0.00017	0.00015	0.00021
	BF_4	N.R.	N/A	N.R.	N/A
	PF_6	N.R.	N/A	N.R.	N/A
	CS	N.R.	N/A	N.R.	N/A

C−H Activation by Potential Step and Application for Other Hydrocarbon Compounds. Above, the potential sweep process could be simplified to a potential-step process to study the electrode surface reactions in situ as well. Potential step experiments provide output of the constant oxidation current under +0.6 V (Figure S5), which confirmed the potential dependency of interface reactions of anaerobic oxidation to methyl radical in NTf_2-based ionic liquids. Methane has the strongest C−H bond in hydrocarbon compounds. C−H bonds in other hydrocarbons which have weaker bonds would be easier to activate by anaerobic oxidation processes discussed in this work. The rate constant (k_3) of hexane is 0.0087, which is 3 times that of methane. And k_3 of pentane is 0.028, which is 10 times that of methane (see the Supporting Information). In the anaerobic oxidation of more than one hydrocarbon compound, such as hexane and pentane, the current should reveal the sum of multiple oxidation processes. The oxidation processes would be more complex than that of methane, and the relative products with long carbon chains should be harder to remove from the electrode surface which could limit the anodic current, with increasing numbers of carbon in the hydrocarbon compounds (see the Supporting Information Figure S8−S9).

CONCLUSION

Our results in this work demonstrate electrochemical anaerobic oxidation of methane to the methyl radical in NTf_2-based ionic liquids at the platinum−[Bmpy][NTf_2] interface. A mechanism is proposed involving multiple steps: (1) electrochemical oxidation of the NTf_2^- anion to generate the NTf_2 radical; (2) formation of the Pt-NTf_2• radical adsorbate at the Pt electrode surface; (3) abstraction of the hydrogen atom from methane by the Pt-NTf_2• radical adsorbate to form the methyl radical; and (4) the methyl radical further attacks the NTf_2^- anion to form CF_3• which generates additional fragmentation products. This mechanism is supported by multiple characterization experiments, including electrochemical (CV, chronoamperometry), NMR, GC/LC−MS and is strongly supported by DFT calculations which show that all the reactions (eqs 1−3) are exergonic in the ionic liquid environment. One of the greatest benefits of the approach described in this work is the chemical versatility combined from the ionic liquids and electrochemistry. IL not only can be solvents, electrolytes, or reaction media but also can be explored as a precursor for the formation of metal catalysts by electrochemistry. For example, the CF_3• radical generated is important for organofluorination.[24] Pt is a high cost metal, but as a heterogeneous electrocatalyst, it can be regenerated and reused. Only the Pt surface is reactive; it can be used in small amounts as in automotive catalytic converters. Our finding is significant as it lays out a principle and strategy that can be used to produce functionalized materials in situ, to subsequently modify these functional groups, and to generate active species, such as metal complexes, through in situ electrochemistry in the ionic liquids. It is also possible that researchers can take this principle to design the catalytic site accordingly based on the need of the reaction which renders the process of designing, optimizing, and rationalizing the structure of heterogeneous catalysis more powerful than it ever was.

ASSOCIATED CONTENT

Supporting Information

The Supporting Information is available free of charge on the ACS Publications website at DOI: 10.1021/acs.jpcc.6b00153.

Experimental details, materials and reagents, electrochemical cells for anaerobic condition, electrochemical gas cell schematic for anaerobic conditions, instruments and methods for testing electrochemical methane sensors, kinetics study experimental details, first cycle peak current vs time, current vs potential, multiple

DOI: 10.1021/acs.jpcc.6b00153
J. Phys. Chem. C 2016, 120, 13466−13473

potential step methods, NMR results, anaerobic oxidation of other hydrocarbon compounds, and computational study methodology (PDF)

AUTHOR INFORMATION

Corresponding Author

*E-mail: zeng@oakland.edu. Tel: 2483702881.

Notes

The authors declare no competing financial interest.

ACKNOWLEDGMENTS

X.Z. is thankful for the NIOSH Grants (R21OH009099 and 1R01OH009644) which provided financial support for this work.

REFERENCES

(1) Hickman, D. A.; Schmidt, L. D. Production of Syngas by Direct Catalytic-Oxidation of Methane. *Science* **1993**, *259*, 343−346.

(2) Scheller, S.; Goenrich, M.; Boecher, R.; Thauer, R. K.; Jaun, B. The Key Nickel Enzyme of Methanogenesis Catalyses the Anaerobic Oxidation of Methane. *Nature* **2010**, *465*, 606−U97.

(3) Periana, R. A.; Mironov, O.; Taube, D.; Bhalla, G.; Jones, C. J. Catalytic, Oxidative Condensation of Ch4 to Ch3cooh in One Step Via Ch Activation. *Science* **2003**, *301*, 814−818.

(4) Osako, T.; Watson, E. J.; Dehestani, A.; Bales, B. C.; Mayer, J. M. Methane Oxidation by Aqueous Osmium Tetroxide and Sodium Periodate: Inhibition of Methanol Oxidation by Methane. *Angew. Chem., Int. Ed.* **2006**, *45*, 7433−7436.

(5) Raghoebarsing, A. A.; et al. A Microbial Consortium Couples Anaerobic Methane Oxidation to Denitrification. *Nature* **2006**, *440*, 918−921.

(6) Beal, E. J.; House, C. H.; Orphan, V. J. Manganese- and Iron-Dependent Marine Methane Oxidation. *Science* **2009**, *325*, 184−187.

(7) Ettwig, K. F.; et al. Nitrite-Driven Anaerobic Methane Oxidation by Oxygenic Bacteria. *Nature* **2010**, *464*, 543−U94.

(8) Knittel, K.; Boetius, A. Anaerobic Oxidation of Methane: Progress with an Unknown Process. *Annu. Rev. Microbiol.* **2009**, *63*, 311−334.

(9) Himes, R. A.; Karlin, K. D. A New Copper-Oxo Player in Methane Oxidation. *Proc. Natl. Acad. Sci. U. S. A.* **2009**, *106*, 18877−18878.

(10) Shilov, A. E.; Shul'pin, G. B. Activation of C-H Bonds by Metal Complexes. *Chem. Rev.* **1997**, *97*, 2879−2932.

(11) Labinger, J. A.; Bercaw, J. E. Understanding and Exploiting C-H Bond Activation. *Nature* **2002**, *417*, 507−514.

(12) Desai, L. V.; Hull, K. L.; Sanford, M. S. Palladium-Catalyzed Oxygenation of Unactivated Sp(3) C-H Bonds. *J. Am. Chem. Soc.* **2004**, *126*, 9542−9543.

(13) Chiappe, C.; Pieraccini, D. Ionic Liquids: Solvent Properties and Organic Reactivity. *J. Phys. Org. Chem.* **2005**, *18*, 275−297.

(14) Welton, T. Room-Temperature Ionic Liquids. Solvents for Synthesis and Catalysis. *Chem. Rev.* **1999**, *99*, 2071−2084.

(15) Xin, B.; Jia, C.; Li, X. Supported Ionic Liquids: Efficient and Reusable Green Media in Organic Catalytic Chemistry. *Curr. Org. Chem.* **2015**, *20*, 616−628.

(16) Wang, Z.; Guo, M.; Baker, G. A.; Stetter, J. R.; Lin, L.; Mason, A. J.; Zeng, X. Methane-Oxygen Electrochemical Coupling in an Ionic Liquid: A Robust Sensor for Simultaneous Quantification. *Analyst* **2014**, *139*, 5140−5147.

(17) Li, F.; Carvalho, S.; Delgado, R.; Drew, M. G. B.; Felix, V. Dimetallic Complexes of Macrocycles with Two Rigid Dibenzofuran Units as Receptors for Detection of Anionic Substrates. *Dalton T* **2010**, *39*, 9579−9587.

(18) Zhang, R. H.; Zhang, X. T.; Hu, S. M. High Temperature and Pressure Chemical Sensors Based on Zr/Zro2 Electrode Prepared by Nanostructured Zro2 Film at Zr Wire. *Sens. Actuators, B* **2010**, *149*, 143−154.

(19) Wang, J. L.; Zhang, Y. X.; Wang, Y. Y.; Xu, R. H.; Sun, Z. H.; Jie, Z. An Innovative Reactor-Type Biosensor for Bod Rapid Measurement. *Biosens. Bioelectron.* **2010**, *25*, 1705−1709.

(20) Marx, A.; Yamamoto, H. Aluminum Bis(Trifluoromethylsulfonyl)Amides: New Highly Efficient and Remarkably Versatile Catalysts for C-C Bond Formation Reactions. *Angew. Chem., Int. Ed.* **2000**, *39*, 178−181.

(21) Sobota, M.; Nikiforidis, I.; Hieringer, W.; Paape, N.; Happel, M.; Steinruck, H. P.; Gorling, A.; Wasserscheid, P.; Laurin, M.; Libuda, J. Toward Ionic-Liquid-Based Model Catalysis: Growth, Orientation, Conformation, and Interaction Mechanism of the [Tf2n](−) Anion in [Bmim][Tf2n] Thin Films on a Well-Ordered Alumina Surface. *Langmuir* **2010**, *26*, 7199−7207.

(22) Sobota, M.; et al. Ionic Liquid Based Model Catalysis: Interaction of [Bmim][Tf2n] with Pd Nanoparticles Supported on an Ordered Alumina Film. *Phys. Chem. Chem. Phys.* **2010**, *12*, 10610−10621.

(23) Tang, Y.; Wang, Z.; Chi, X.; Sevilla, M. D.; Zeng, X. In Situ Generated Platinum Catalyst for Methanol Oxidation Via Electrochemical Oxidation of Bis(Trifluoromethylsulfonyl)Imide Anion in Ionic Liquids at Anaerobic Condition. *J. Phys. Chem. C* **2016**, *120*, 1004−1012.

(24) Jiang, L.; Qian, J.; Yi, W.; Lu, G.; Cai, C.; Zhang, W. Direct Trifluoromethylthiolation and Perfluoroalkylthiolation of C(sp^2)-H Bonds with CF_3SO_2Na and R_fSO_2Na. *Angew. Chem., Int. Ed.* **2015**, *54*, 14965−14969.

(25) *Spartan10*; Wavefunction, Inc., 2010.

(26) Frisch, M. J.; Trucks, G. W.; Schlegel, H. B.; Scuseria, G. E.; Robb, M. A.; Cheeseman, J. R.; Scalmani, G.; Barone, V.; Mennucci, B.; Petersson, G. A. et al. *Gaussian 09*, revision B.01; Gaussian, Inc.: Wallingford, CT, 2009.

(27) Williams, D. B.; Stoll, M. E.; Scott, B. L.; Costa, D. A.; Oldham, W. J., Jr. Coordination Chemistry of the Bis(Trifluoromethylsulfonyl)-Imide Anion: Molecular Interactions in Room Temperature Ionic Liquids. *Chem. Commun.* **2005**, 1438−1440.

(28) Belyaev, V. D.; Gal'vita, V. V.; Gorelov, V. P.; Sobyanin, V. A. Oxidation of Methane over Platinum in a Solid Proton-Conducting Electrolyte Cell. *Catal. Lett.* **1995**, *30*, 151−158.

(29) Kertesz, V.; Chambers, J. Q.; Mullenix, A. N. Chronoamperometry of Surface Confined Redox Couples for Irreversible Two-Step and Three-Step Consecutive Reaction Mechanisms. *Anal. Chem.* **1999**, *71*, 3905−3909.

(30) Kertesz, V.; Chambers, J. Q.; Mullenix, A. N. Chronoamperometry of Surface-Confined Redox Couples. Application to Daunomycin Adsorbed on Hanging Mercury Drop Electrodes. *Electrochim. Acta* **1999**, *45*, 1095−1104.

(31) Kakutani, T.; Osakai, T.; Senda, M. A Potential-Step Chronoamperometric Study of Ion Transfer at the Water Nitrobenzene Interface. *Bull. Chem. Soc. Jpn.* **1983**, *56*, 991−996.

(32) Inzelt, G. Simultaneous Chronoamperometric and Quartz Crystal Microbalance Studies of Redox Transformations of Polyaniline Films. *Electrochim. Acta* **2000**, *45*, 3865−3876.

(33) Paulse, C. D.; Pickup, P. G. Chronoamperometry of Polypyrrole - Migration of Counterions and Effect of Uncompensated Solution Resistance. *J. Phys. Chem.* **1988**, *92*, 7002−7006.

(34) Held, A. M.; Manthorne, K. C.; Pacey, P. D.; Reinholdt, H. P. Individual Rate Constants of Methyl Radical Reactions in the Pyrolysis of Dimethyl Ether. *Can. J. Chem.* **1977**, *55*, 4128−4134.

(35) Washida, N.; Bayes, K. D. The Reactions of Methyl Radicals with Atomic and Molecular Oxygen. *Int. J. Chem. Kinet.* **1976**, *8*, 777−794.

(36) Lagrost, C.; Carrié, D.; Vaultier, M.; Hapiot, P. Reactivities of Some Electrogenerated Organic Cation Radicals in Room-Temperature Ionic Liquids: Toward an Alternative to Volatile Organic Solvents? *J. Phys. Chem. A* **2003**, *107*, 745−752.

(37) Weingärtner, H.; Sasisanker, P.; Daguenet, C.; Dyson, P. J.; Krossing, I.; Slattery, J. M.; Schubert, T. The Dielectric Response of Room-Temperature Ionic Liquids: Effect of Cation Variation. *J. Phys. Chem. B* **2007**, *111*, 4775−4780.

DOI: 10.1021/acs.jpcc.6b00153
J. Phys. Chem. C 2016, 120, 13466−13473

(38) Yannoni, C. S.; Dailey, B. P.; Ceasar, G. P. Studies of Chemical Shift Anisotropy in Liquid Crystal Solvents. Iv. Results for Some Fluorine Compounds. *J. Chem. Phys.* **1971**, *54*, 4020−4023.
(39) Cobos, C. J.; Capparelli, A. L. Correlations between F-19 Nmr Chemical-Shifts and Bond-Dissociation Energies, Enthalpies of Formation and Group Electronegativities. *J. Fluorine Chem.* **1995**, *70*, 155−162.
(40) Knowles, H. S.; Parsons, A. F.; Pettifer, R. M.; Rickling, S. Desulfonylation of Amides Using Tributyltin Hydride, Samarium Diiodide or Zinc/Titanium Tetrachloride. A Comparison of Methods. *Tetrahedron* **2000**, *56*, 979−988.
(41) Knowles, H.; Parsons, A. F.; Pettifer, R. M. Desulfonylation of Amides Using Samarium Iodide. *Synlett* **1997**, *1997*, 271−272.
(42) Shainyan, B. A.; Meshcheryakov, V. I.; Sterkhova, I. V. A Convenient Synthesis and Structure of N-Trifluoromethylsulfonylamidines. *Tetrahedron* **2015**, *71*, 7906−7910.
(43) Zhu, S.; He, P. Study on the Fluorine-Containing Reactive Intermediates and Their Application in the Organic Synthesis. *Curr. Org. Chem.* **2004**, *8*, 97−112.
(44) Ettwig, K. F.; Butler, M. K.; Le Paslier, D.; Pelletier, E.; Mangenot, S.; et al. Nitrite-Driven Anaerobic Methane Oxidation by Oxygenic Bacteria. *Nature* **2010**, *464*, 543−548.
(45) Mayr, S.; Latkoczy, C.; Kruger, M.; Gunther, D.; Shima, S.; Thauer, R. K.; Widdel, F.; Jaun, B. Structure of an F430 Variant from Archaea Associated with Anaerobic Oxidation of Methane. *J. Am. Chem. Soc.* **2008**, *130*, 10758−10767.
(46) Jafarian, M.; Mahjani, M. G.; Heli, M. G.; Gobal, F.; Heydarpoor, M. Electrocatalytic Oxidation of Methane at Nickel Hydroxide Modified Nickel Electrode in Alkaline Solution. *Electrochem. Commun.* **2003**, *5*, 184−188.
(47) Baldelli, S. Surface Structure at the Ionic Liquid-Electrified Metal Interface. *Acc. Chem. Res.* **2008**, *41*, 421−431.

DOI: 10.1021/acs.jpcc.6b00153
J. Phys. Chem. C 2016, 120, 13466−13473